

A Meta surface Superstrate for Mutual Coupling Reduction of Large Antenna Arrays

Abhishek Das¹, Niranjan Mishra², Manoranjan Sahoo³, Rudra Prasad Nanda⁴

¹Department of Electronics & Communication Engineering, Raajdhani Engineering College, Bhubaneswar, Odisha

²Department of Electronics & Communication Engineering, NM Institute Engineering & Technology, Bhubaneswar, Odisha

³Department of Electronics & Communication Engineering, Capital Engineering College, Bhubaneswar, Odisha

⁴Department of Electronics & Communication Engineering, Aryan Institute of Engineering and Technology, Bhubaneswar, Odisha

ABSTRACT In this paper, a ϵ -negative metasurface superstrate is proposed for mutual coupling reduction of large antenna arrays. Unlike the previous decoupling metasurface works that are mostly confined to two-ports antennas, the proposed decoupling superstrate can be extended to massive multiple-input multiple-output (MIMO) systems. A 4 × 4 antenna array is used as an example to illustrate the decoupling performance of the proposed metasurface. With the decoupling metasurface, the worst mutual coupling of the antenna array is improved by 8 dB over the operation bandwidth with a maximum mutual coupling reduction of 25 dB. Moreover, the decoupling metasurface also help restore the radiation patterns, bring down the active voltage standing wave ratio, and broaden the bandwidth of the array.

Keywords: Array, metasurface, mutual coupling reduction, superstrate.

I. INTRODUCTION

Modern wireless communication systems demand enhancements of data rate and reliability. In order to fulfill these requirements, multiple-input multiple-output (MIMO) systems are used ubiquitously in various applications [1]–[3]. Due to space limitation and aesthetic reasons, compact array antennas are often used, which makes mutual coupling inevitable [4]. Mutual coupling can result in high sidelobes, gain reduction, large voltage standing wave ratio (VSWR), etc., which in turn cause a significant degradation of the MIMO performance [5]. Over the last decades, a lot of research work has been devoted to mutual coupling reductions [6]–[25]. Different decoupling techniques have been proposed, such as defected ground structure (DGS) [8], parasitic element [9], electromagnetic bandgap (EBG) [10]–[12], neutralization line [13], asymmetric coplanar wall [14], topology optimization [15], array-antenna decoupling surface (ADS) [16], decoupling ground [17], near-field resonator [18], polarization diversity [19], [20], split ring resonator (SRR) based metasurface [21]–[27] and T-shaped decoupling feeding network [28]. All the above-mentioned

methods can effectively mitigate the mutual coupling. Nevertheless, most of them are limited to decoupling of two-port antennas. Except for [16]–[18], most of the decoupling techniques are difficult to be extended to large antenna arrays.

In this work, we focus on the metasurface based decoupling technique. Unlike the previous SRR based metasurface (with negative permeability μ and positive permittivity ϵ) works that are mostly confined to two-port antennas [21]–[25], we propose a new metasurface superstrate (with negative ϵ and positive μ) for decoupling of large antenna arrays. Noted that it is relatively easy to achieve high isolation of a two-port antenna (1×2 array) or 2×2 array. However, it is not a trivial task to achieve high isolation for larger arrays (e.g., 4×4 array) in that the mutual couplings between the inner and outer array elements make the overall decoupling a challenging task. For example, the decoupling metasurface in [22] becomes less effective when applied to large planar arrays directly, because its equivalent permeability is negative only within a small angular range over the array aperture. In order to enable decoupling for large arrays, the proposed metasurface in this work achieves negative permittivity over large angular range and thus can reduce the mutual coupling effectively over the whole planar array, as explained in the next section.

As a demonstration, a 4×4 array¹ with center-to-center (edge-to-edge) separation of $0.43\lambda_0$ ($0.19\lambda_0$) at 5.8 GHz is designed to show the effectiveness of the proposed decoupling metasurface. Thanks to the proposed decoupling metasurface, more than 8 dB isolation enhancement is achieved over the operation bandwidth (with a maximum mutual coupling reduction of 25 dB at the center frequency of 5.8 GHz). In addition, it is shown that the decoupling metasurface also helps broaden the operation bandwidth of the array, restore the radiation patterns for good coverage, and bring down VSWR for MIMO precoding.

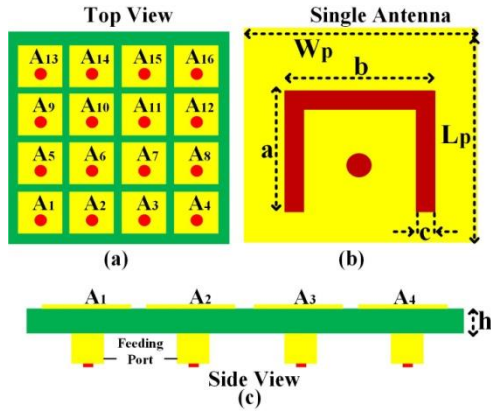


FIGURE 1. 4×4 antenna array: (a) top view, (b) single antenna with U-shaped slot, and (c) side view.

II. ANTENNA ARRAY WITH DECOUPLING SUPERSTRATE

In this work, we propose a decoupling metasurface superstrate for large planar arrays. To show the applicability of the proposed decoupling superstrate to massive MIMO array, a 4×4 array antenna working at 5.8 GHz is designed, as shown in Fig. 1. The array is printed on a substrate of RO4350B with a size of 110 mm \times 110 mm \times 1.52 mm and dielectric constant of 3.48. The center-to-center (edge-to-edge) separation of the array is $0.43\lambda_0$ ($0.19\lambda_0$). The patch antennas are marked as A1- A16 as shown in Fig. 1(a). The length and width of the rectangular patches are denoted as L_p and W_p , respectively, as marked in Fig. 1(b). A capacitive U-shaped slot is inserted around the feeding point (i.e., the red dot in Fig. 1(b)) of each patch element to improve the impedance matching [29].

The metasurface superstrate ($L_s \times L_s \times H_s$) consisting of 13×13 unit cells is fabricated on the Taconic-TLT 6 with a dielectric constant of 2.65 (The number of cells becomes insensitive to the decoupling performance once it is larger than 10 and the decoupling superstrate is larger than the array. We choose 13×13 unit cells in this work so that the decoupling superstrate is slightly larger than the array.) The structure of the unit cell is presented in Fig. 2(a). The dimension values of the optimized unit cell structure are listed in Table 1.

¹If the decoupling superstrate can work for 4×4 arrays, it can certainly be extended to larger arrays.

TABLE 1. Parameters values.

Parameters	Values (mm)	Parameters	Values (mm)
L_1	8.50	L_2	3
L_3	6	L_4	2.50
L_5	8.50	L_6	5
L_7	3	L_8	2.25
L_{sub}	110	g_1	1
g_2	0.25	L_p	12.4
W_p	12.3	a	4
h_1	3.5	c	0.40
h_2	2	n	0.65
b	3.80	H	1.5
h	1.52	L_s	120

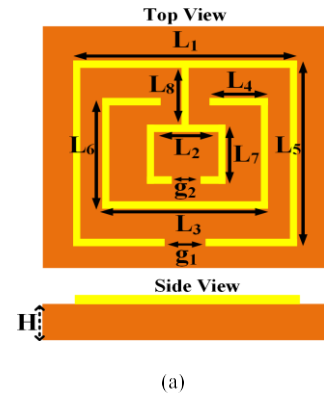


FIGURE 2. (a) Structure of the unit cell; (b) unit cell simulation model.

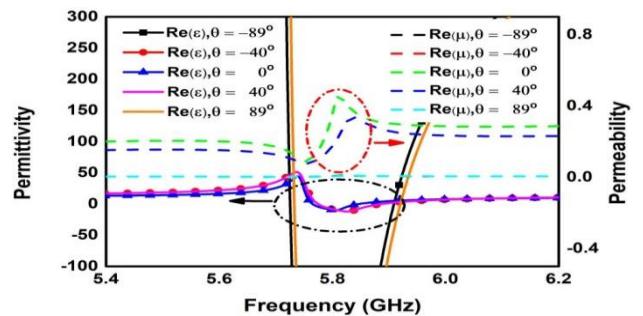


FIGURE 3. Permittivity and permeability of the unit cell at different incident angles.

The CST microwave studio is used for simulations in this work. Fig. 2(b) shows the simulation model of the unit cell. Permeability and permittivity values are extracted using the method proposed in [30]. It is observed from Fig. 3 that the metasurface exhibits negative permittivity ϵ (and positive permeability μ) over a wide angular range ($-89^\circ \leq \theta \leq 89^\circ$).

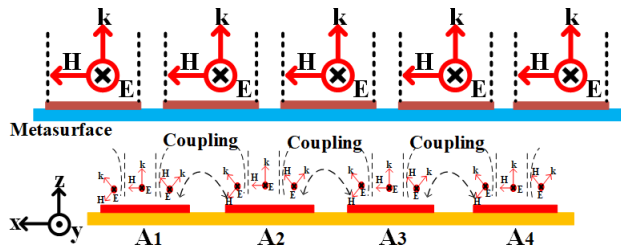


FIGURE 4. Illustration of field distribution of the antenna array.

The mutual coupling of the array is illustrated in Fig. 4. The metasurface with negative ϵ creates an equivalent media with an imaginary tangential wave number $k_t = k_0 \sqrt{-|\mu| \cdot |\epsilon|} = jk_0 \sqrt{|\mu| \cdot |\epsilon|}$, which turns the tangential surface wave into evanescent wave $A_0 e^{jk_x x} = A_0 e^{-k_0 \sqrt{|\mu| \cdot |\epsilon|} x}$. In this way, the mutual coupling caused by the surface wave in the angular range of $-89^\circ \leq \theta \leq 89^\circ$ can be effectively suppressed, whereas the angular range of negative μ produced by the SRRs in [23] is less than $-40^\circ \leq \theta \leq 40^\circ$, i.e., much smaller than the angular range of negative ϵ in this work.

For the given array configuration [cf. Fig. 1(a)] with center-to-center (edge-to-edge) separation of $0.43\lambda_0$ ($0.19\lambda_0$), the H-plane coupling dominates (i.e., about -12 dB). Therefore, we orientate the decoupling metasurface so that it can effectively mitigate the H-plane coupling (e.g., mutual coupling between elements 1 and 2), whereas the E-plane coupling (e.g., mutual coupling between elements 1 and 5) can be further reduced by optimizing the patch shape, as further discussed in the next section. This ensures the applicability of the decoupling scheme to massive MIMO arrays.

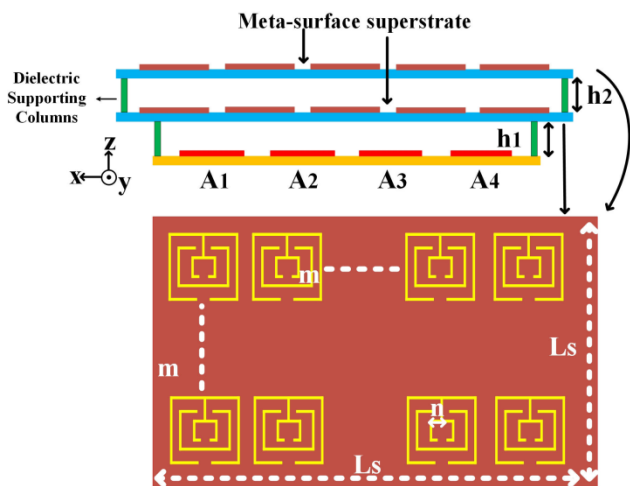
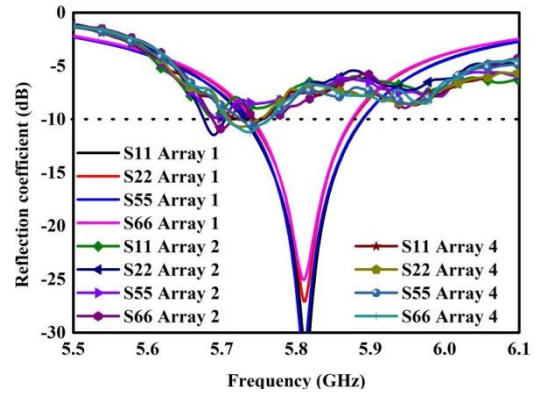
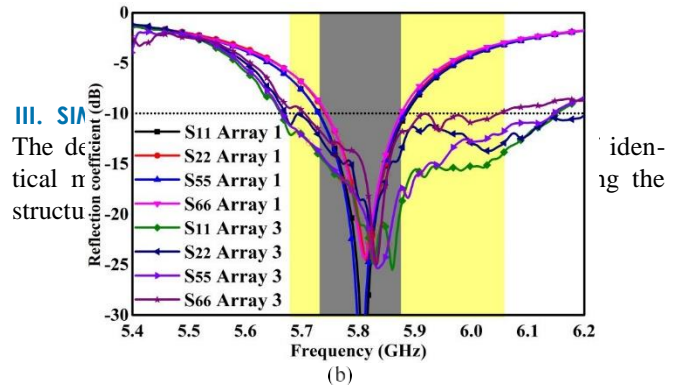


FIGURE 5. Illustration of the decoupling superstrate.



(a)



(b)

FIGURE 6. Reflection coefficients of (a) array 1 and array 2 and array 4 (b) array 1 and array 3.

of the decoupling superstrate and the U-shaped slot [see Fig. 1(b)]. The reflection coefficients of the antenna arrays without decoupling superstrate and U-shaped slots (Array 1), without decoupling superstrate yet with U-slots (Array 2), with both decoupling superstrate and U-slots (Array 3) and with decoupling superstrate yet without U-slots (Array 4) are compared in Fig. 6. Note that due to the geometric symmetry of the array, only the S-parameters corresponding to antennas A_1 , A_2 , A_5 and A_6 are shown here. Fig. 6(a) shows the comparisons of the reflection coefficients of Array 1, Array 2 and Array 4, whereas Fig. 6(b) shows that of Array 1 and Array 3. It is observed from Fig. 6(a) that using the U-shaped slots or the decoupling superstrate alone cannot match the antenna well. It can be seen from Fig. 6(b) that the U-shaped slot improves the impedance matching while the decoupling superstrate also helps broaden the bandwidth of Array 3, implying the U-shaped slots should actually be used in combination with the decoupling metasurface to achieve good matching. Note that one metasurface layer can also reduce the mutual coupling for the reasons mentioned in the previous section. Nevertheless, it is found that by using two layers of metasurfaces (cf. Fig. 7), better reflection coefficients can be achieved at the expense of slightly increased profile (about 2 mm) and increasing the number of layers beyond two hardly improve the matching. Therefore, the double-layer decoupling structure (cf. Fig. 5) is chosen in this work. Note that the cost of fabricating two identical

metasurfaces is only slightly higher than that of fabricating one metasurface.

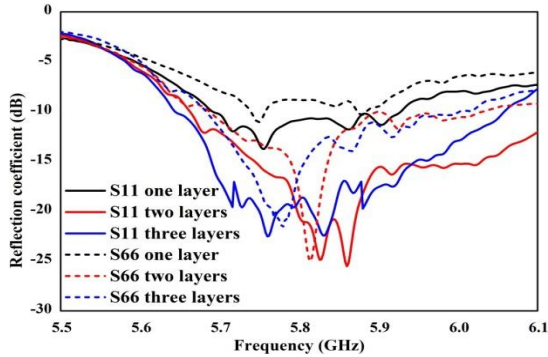


FIGURE 7. Reflection coefficients of proposed array with one layer of metasurface, proposed array with two layers of metasurfaces and proposed array with three layers of metasurfaces.

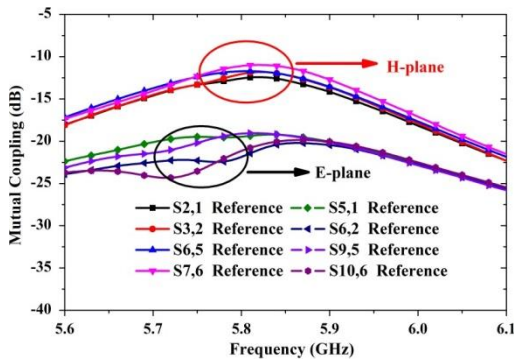


FIGURE 8. Comparison of E-plane and H-plane couplings of the reference array.

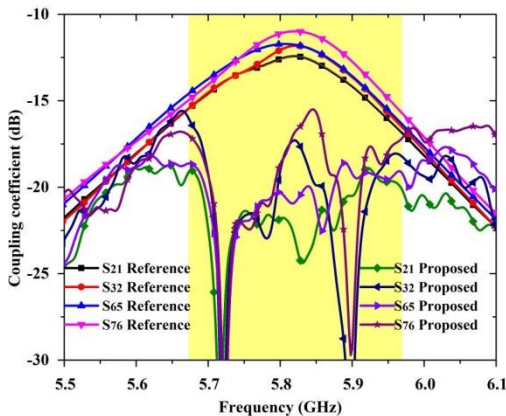


FIGURE 9. Worst mutual couplings of the reference and proposed arrays.

The decoupling effect of the proposed metasurface super-

strate is shown in Fig. 9 by comparing the mutual couplings of the reference array (Array 1) and the proposed array (Array 3). Note that for clear exhibition, only the worst mutual couplings of the corresponding arrays are shown here. Given the array with center-to-center (edge-to-edge) separation of $0.43\lambda_0$ ($0.19\lambda_0$), the H-plane coupling (i.e., the mutual coupling between horizontally adjacent array elements) dominates. From Fig. 8, the mutual couplings between vertically and diagonally adjacent elements are smaller than that of the horizontally adjacent elements. It is observed that the worst coupling of Reference array is around 11 dB at 5.8 GHz, whereas with the decoupling superstrate, the worst mutual coupling of the proposed array is improved by at least 8 dB over the entire bandwidth (with a maximum reduction of more than 25 dB at the center frequency of 5.8 GHz).

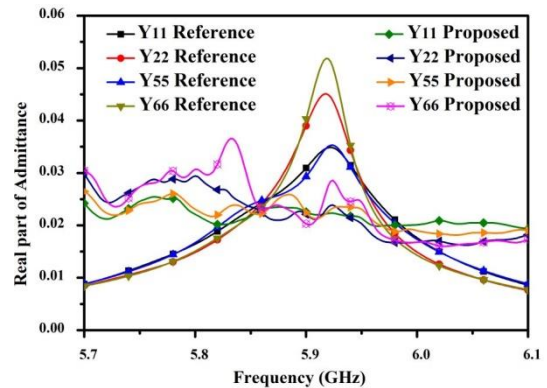


FIGURE 10. Self-admittances of the reference and proposed arrays.

The bandwidth enhancement of the decoupling superstrate can be further illustrated from the admittance curves as shown in Fig. 10. Reference array has sharp slopes near the center frequency, while the slope of the proposed array is much flatter. Next, we further illustrate the decoupling mechanism by examining the field distributions with and without the decoupling superstrate.

Fig. 11 shows the E-field distributions of the reference and proposed arrays at 5.8 GHz when Antenna A_1 or Antenna A_6 is excited. It is observed from Fig. 10(a) that without the decoupling superstrate, there is strong mutual coupling between the antenna elements. It can be seen from Fig. 10(b) that with the decoupling superstrate, the mutual coupling can be greatly suppressed.

Fig. 12 shows the total antenna efficiencies of the reference and proposed arrays. It is observed that the total efficiencies of elements A_1 , A_2 , A_5 and A_6 of Reference array at 5.8 GHz are around 77%, 65%, 71%, and 60%, respectively, whereas their counterparts of Proposed array are all about 76%–77% at 5.8 GHz thanks to the reduced coupling losses. Moreover, as can be seen, decoupling superstrate also broadens the array's bandwidth [see also Fig. 6(b)]. The realized gains of the four antenna elements are shown in Fig. 13. As expected, the gain improves as the mutual coupling reduces [31]. Comparisons of the envelope correlation coefficients (ECCs) [32] calculated from the simulated radiation patterns in CST are shown in Fig. 14. It can be seen that the ECCs of the proposed array are lower than that of the reference array over the entire bandwidth.

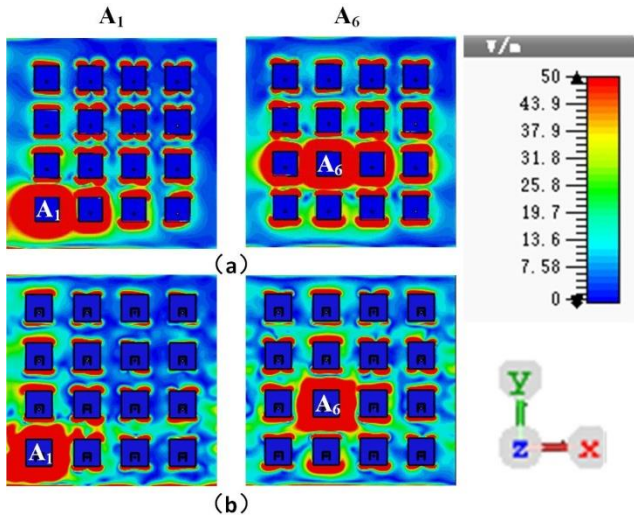


FIGURE 11. E-fields of (a) the reference array and (b) proposed array at 5.8 GHz. The left column corresponds to the case where Antenna 1 is excited, while the right column corresponds to the case where antenna 6 is excited.

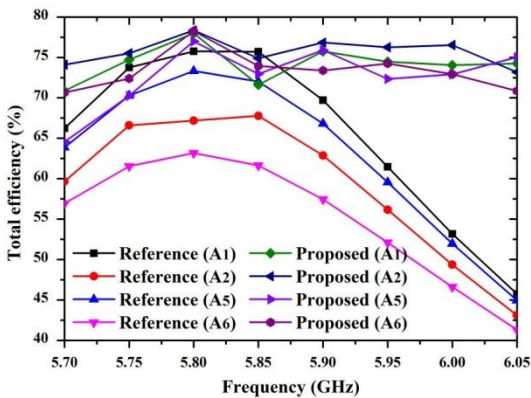


FIGURE 12. Total antenna efficiencies of the reference and proposed arrays.

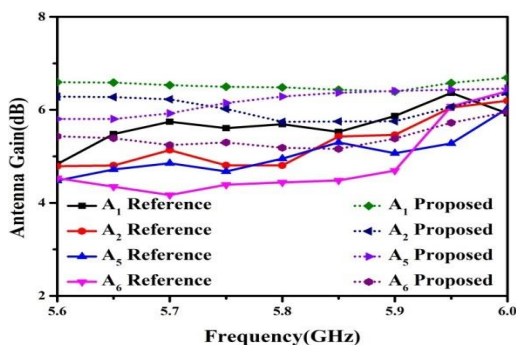


FIGURE 13. Realized gains of the reference and proposed arrays.

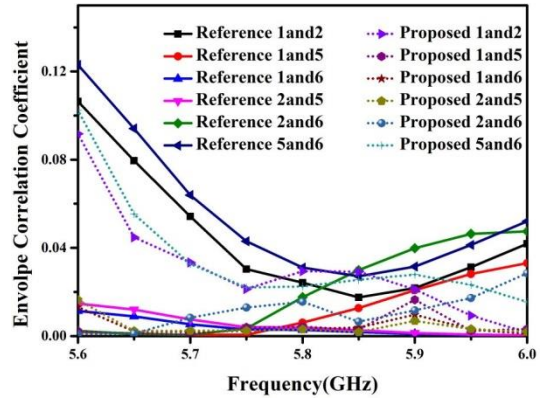


FIGURE 14. Envelope correlation coefficients of the reference and proposed arrays.

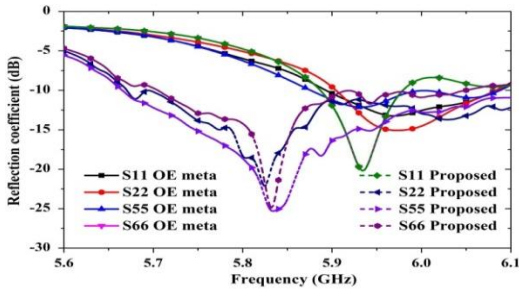
OE meta so that it has the same size and height. (Note that [24] also employed a double-layer structure.) A comparison of both metasurfaces on the same array is shown in Fig. 15. From the reflection coefficients in Fig. 15(a), there is some frequency offset of the array with the OE meta. Since the main purpose is to compare their decoupling effects on the 4 4 array, their exact resonating frequencies are not important. Figs. 15(b) and (c) show that the proposed array achieves overall much lower mutual coupling than that with the OE meta at their operating frequencies. This example indicates that decoupling superstrate that works for 1 2 antenna array (as demonstrated in [24]) may not be directly applicable to larger arrays. By contrast, since the decoupling metasurface can work for a 4 4 array, it will also be feasible for larger arrays.

To further motivate the decoupling metasurface, we compare the active voltage standing wave ratios (VSWRs) of the reference and proposed arrays. To that end, we take similar assumptions as that in [16] [17]. Suppose the 4 4 array is used at an access point (AP) that serves four user equipments (UEs) simultaneously, forming a 4 16 MIMO system in the downlink mode. At the AP, four random binary phase shift keying (BPSK) data streams are precoded by using the zero-forcing (ZF) algorithm. For simplicity, we assume Rayleigh fading MIMO channel \mathbf{H} , which is a 4 16 matrix with independent and identically distributed (i.i.d.) complex Gaussian random variables as its entries. The ZF precoder can then be expressed as $\mathbf{H}^{\dagger} \mathbf{H}^H \mathbf{H}^{-1} \mathbf{H}^H$, where the superscripts \dagger and H represent pseudo-inverse and conjugate transpose, respectively. Denote the raw BPSK data streams at an arbitrary time sample as a 4 1 column vector \mathbf{s} . The precoded data stream can be expressed as $\mathbf{x} = \mathbf{H}^{\dagger} \mathbf{s}$. The active reflection at the n th AP antenna can be calculated as

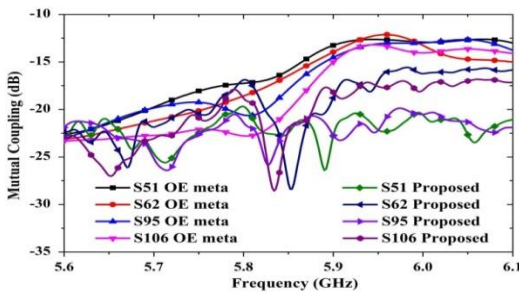
$$\sum_{m=1}^m$$

To illustrate the difference between this work and the meta- surface in Optics Express [24] (which is represented as OE meta in the sequel), a frequency scaling is performed on the

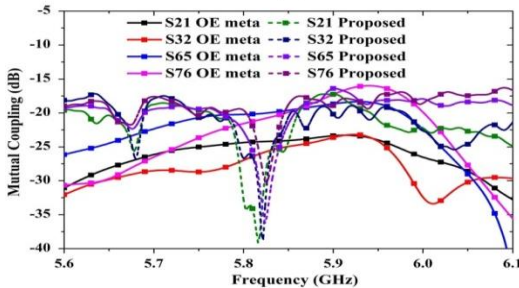
$\Gamma_n = \frac{1}{N} \sum_{m=1}^N S_{nm} x_m$ [33], where S_{nm} is the S-parameter x_m is the m th entry of the vector \mathbf{x} . Note that the minimum value of x_m is limited to 0.1 to avoid the singularity problem caused by very small excitations. The active VSWR at the n th AP antenna can be calculated as $(1 + |\Gamma_n|) / (1 - |\Gamma_n|)$.



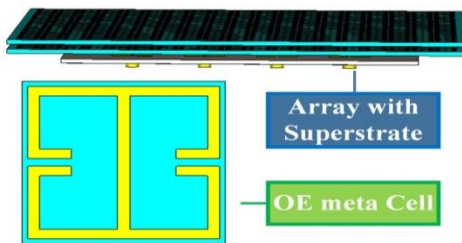
(a)



(b)



(c)



(d)

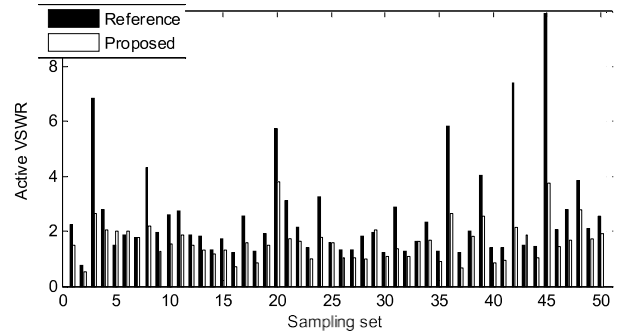


FIGURE 16. Active VSWRs of Reference array and Proposed array.

FIGURE 15. (a) Reflection coefficient of the proposed array and OE metaarray (b) E-plane mutual coupling of proposed array and OE meta array (c) H-plane mutual coupling of proposed array and OE meta array (d) topview of OE meta cell and array with OE meta superstrate.

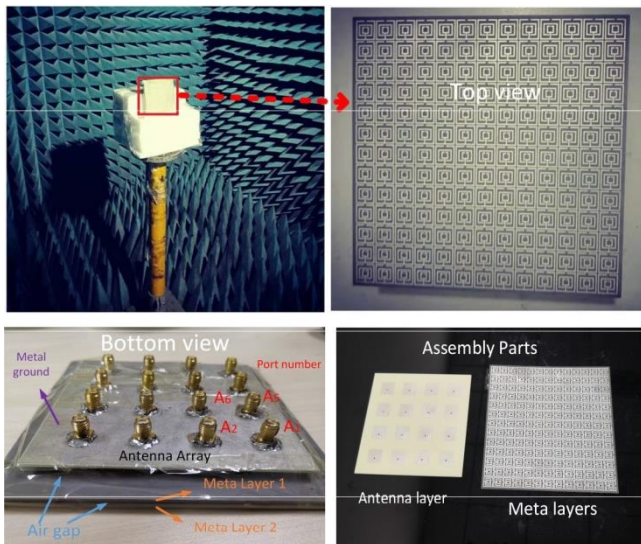


FIGURE 17. Fabricated prototype in an anechoic chamber for measurements with top and bottom view as well as assembly parts.

Fig. 16 compares the worst VSWRs among the 16 AP antennas in the frequency range of 575.9 GHz for the reference and proposed arrays under 50 random channel realizations (excitations). As can be seen, the decoupling metasurface can suppress the active VSWR effectively.

IV. MEASUREMENTS

To further verify the proposed decoupling superstrate, a prototype of the proposed antenna array is fabricated and measured in an anechoic chamber as shown in Fig. 17.

Simulated and measured reflection coefficients and mutual couplings of the proposed antenna array are shown in Figs. 18 and 19, respectively. As can be seen, there are some discrepancies between the measured and simulated S-parameters. These are mainly due to imperfect soldering of the feeding ports and assembling of the array and metasurface superstrate. It is found that the measured resonating frequencies of the array varies as we adjust the superstrate height above it. Nevertheless, the measured reflection and mutual coupling coefficients are sufficiently small, implying good matching and decoupling of the fabricated prototype.

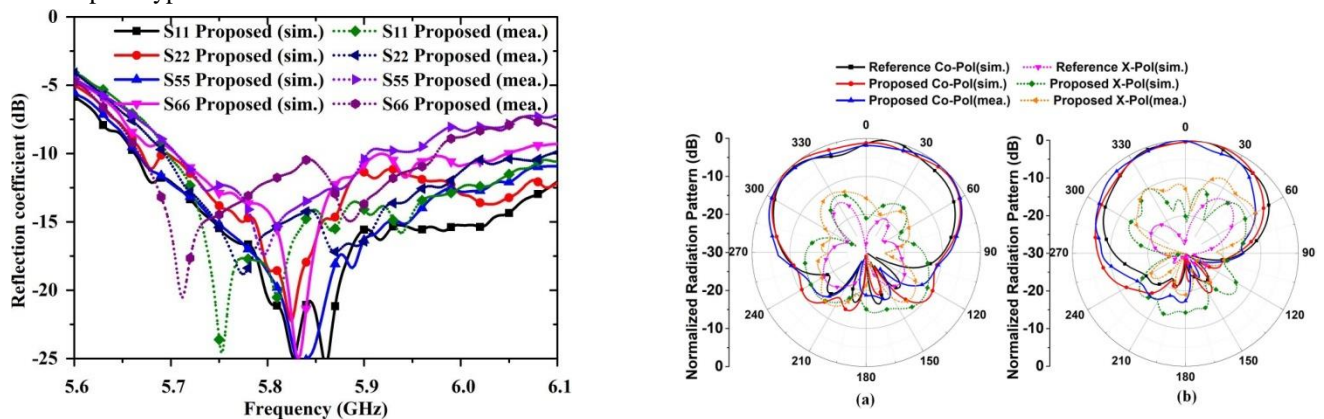


FIGURE 18. Simulated (sim.) and measured (mea.) reflection coefficients of proposed array.

FIGURE 19. Simulated and measured mutual couplings of proposed array.

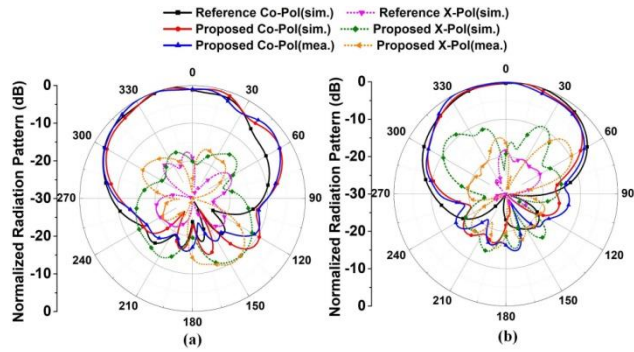


FIGURE 20. Radiation pattern of antenna (A₁) at 5.8 GHz (a) H-plane (b) E-plane.

Figs. 20-23 show the simulated and measured radiation patterns of array elements A₁, A₂, A₅ and A₆ of the reference and proposed arrays, respectively. Good agreements are observed for the measured and simulated radiation patterns for Proposed array. The small discrepancies are mainly attributed to misalignment in the measurements, manufacturing tolerance and imperfect soldering. It can be seen by comparing the radiation patterns of the reference and

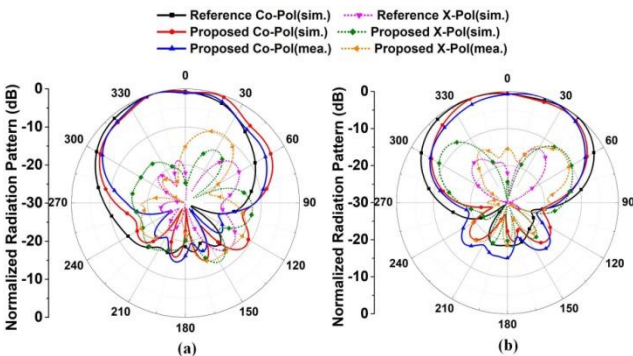


FIGURE 21. Radiation pattern of antenna (A₂) at 5.8 GHz (a) H-plane (b) E-plane.

proposed arrays that the decoupling metasurface helps restore the radiation patterns of the coupled elements. For instance, due to the strong mutual coupling, the main beam

of element A₁ in the corner of the reference array is tilted outwards (away from the array's broadside). Since element A₆ is in the middle of the Reference array, its main beam is not tilted, yet its H-plane pattern becomes irregular and its E-plane pattern is broadened. With effective mutual coupling reduction, the radiation patterns of elements A₁, A₂, A₅ and A₆ of the proposed array are restored to some extent. This ensures good coverage of the decoupled array.

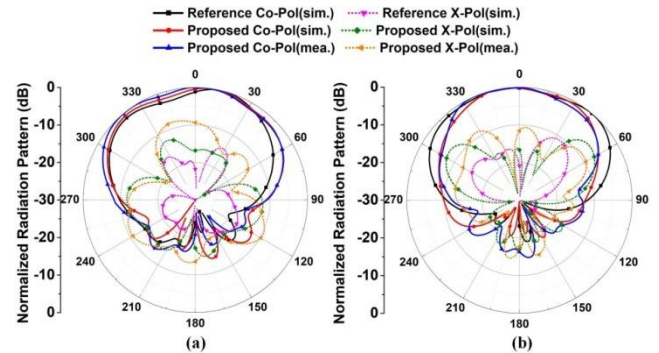


FIGURE 22. Radiation pattern of antenna (A₅) at 5.8 GHz (a) H-plane

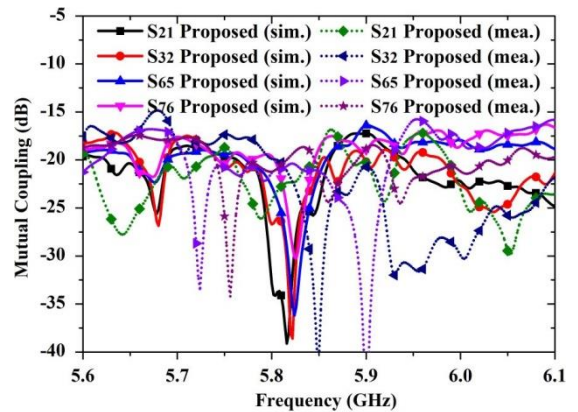


FIGURE 23. Radiation pattern of antenna (A₆) at 5.8 GHz

V. CONCLUSION

In this paper, a double-layer metasurface was proposed for mutual coupling reduction of massive MIMO antennas. The periodic arrangement of unit cells exhibited negative permittivity (and positive permeability), which turned the surface wave into evanescent tangential wave, as pointed by the previous literature. However, unlike the previous decoupling metasurface works that were confined to two-port antennas, extra cares were exerted in optimizing the parameters of the metasurface so that it could suppress the mutual coupling in a wide angular range. Hence, the proposed decoupling metasurface could be applied to large planar array. A 4 × 4 antenna array was designed for experimental demonstration. It was shown that the mutual coupling caused by surface waves could be greatly suppressed by placing the decoupling metasurface above the 4 × 4 array. With the proposed decoupling metasurface superstrate, the worst mutual coupling is improved by at least 8 dB over the entire bandwidth with a maximum mutual coupling reduction of more than 25 dB at the center frequency of 5.8 GHz. Moreover, it was shown that the decoupling superstrate also helped broaden the bandwidth and restore the radiation patterns of the antenna array.

×

REFERENCES

- [1] R. He, R. He, B. Ai, G. L. Stüber, G. Wang, and Z. Zhong, "Geometrical-based modeling for millimeter-wave MIMO mobile-to-mobile channels," *IEEE Trans. Veh. Technol.*, vol. 67, no. 4, pp. 2828–2863, Apr. 2018.
- [2] K. Guan, Z. Zhong, J. I. Alonso, and C. Briso-Rodriguez, "Measurement of distributed antenna systems at 2.4 GHz in a realistic subway tunnel environment," *IEEE Trans. Veh. Technol.*, vol. 61, no. 2, pp. 834–837, Feb. 2012.
- [3] M. Li, X. Chen, A. Zhang, and A. A. Kishk, "Dual-polarized broadband base station antenna backed with dielectric cavity for 5G communications," *IEEE Antennas Wireless Propag. Lett.*, vol. 18, no. 10, pp. 2051–2055, Oct. 2019.
- [4] M. S. Sharawi, "Current misuses and future prospects for printed multiple-input, multiple-output antenna systems [wireless corner]," *IEEE Antennas Propag. Mag.*, vol. 59, no. 2, pp. 162–170, Apr. 2017.
- [5] X. Chen, S. Zhang, and Q. Li, "A review of mutual coupling in MIMO systems," *IEEE Access*, vol. 6, pp. 24706–24719, 2018.
- [6] I. Nadeem and D.-Y. Choi, "Study on mutual coupling reduction technique for MIMO antennas," *IEEE Access*, vol. 7, pp. 563–586, 2019.
- [7] C.-Y. Chiu, F. Xu, S. Shen, and R. D. Murch, "Mutual coupling reduction of rotationally symmetric multiport antennas," *IEEE Trans. Antennas Propag.*, vol. 66, no. 10, pp. 5013–5021, Oct. 2018.
- [8] C.-M. Luo, J.-S. Hong, and L.-L. Zhong, "Isolation enhancement of a very compact UWB-MIMO slot antenna with two defected ground structures," *IEEE Antennas Wireless Propag. Lett.*, vol. 14, pp. 1766–1769, Apr. 2015.
- [9] B. K. Lau and J. B. Andersen, "Simple and efficient decoupling of compact arrays with parasitic scatterers," *IEEE Trans. Antennas Propag.*, vol. 60, no. 2, pp. 464–472, Feb. 2012.
- [10] H. Yi and S. Qu, "A novel dual-band circularly polarized antenna based on electromagnetic band-gap structure," *IEEE Antennas Wireless Propag. Lett.*, vol. 12, pp. 1149–1152, Sep. 2013.
- [11] Q. Li, A. P. Feresidis, M. Mavridou, and P. S. Hall, "Miniaturized double-layer EBG structures for broadband mutual coupling reduction between UWB monopoles," *IEEE Trans. Antennas Propag.*, vol. 63, no. 3, pp. 1168–1171, Mar. 2015.
- [12] A. Pirhadi, H. Bahrami, and A. Mallahzadeh, "Electromagnetic band gap (EBG) superstrate resonator antenna design for monopulse radiation pattern," *Appl. Comput. Electromagn. Soc. J.*, vol. 27, no. 11, pp. 908–917, 2012.
- [13] S. Wang and Z. Du, "Decoupled dual-antenna system using crossed neutralization lines for LTE/WWAN smartphone applications," *IEEE Antennas Wireless Propag. Lett.*, vol. 14, pp. 523–526, Nov. 2015.
- [14] H. Qi, L. Liu, X. Yin, H. Zhao, and W. J. Kulesza, "Mutual coupling suppression between two closely spaced microstrip antennas with an asymmetrical coplanar strip wall," *IEEE Antennas Wireless Propag. Lett.*, vol. 15, pp. 191–194, Jun. 2016.
- [15] S.-H. Zhu, X.-S. Yang, J. Wang, N.-S. Nie, and B.-Z. Wang, "Mutual coupling reduction of 45° dual-polarized closely spaced MIMO antenna by topology optimization," *IEEE Access*, vol. 8, pp. 29089–29098, 2020.
- [16] K.-L. Wu, C. Wei, X. Mei, and Z.-Y. Zhang, "Array-antenna decoupling surface," *IEEE Trans. Antennas Propag.*, vol. 65, no. 12, pp. 6728–6738, Dec. 2017.
- [17] S. Zhang, X. Chen, and G. F. Pedersen, "Mutual coupling suppression with decoupling ground for massive MIMO antenna arrays," *IEEE Trans. Veh. Technol.*, vol. 68, no. 8, pp. 7273–7282, Aug. 2019.
- [18] M. Li, B. G. Zhong, and S. W. Cheung, "Isolation enhancement for MIMO patch antennas using near-field resonators as coupling-mode transducers," *IEEE Trans. Antennas Propag.*, vol. 67, no. 2, pp. 755–764, Feb. 2019.
- [19] C. F. Ding, X. Y. Zhang, C.-D. Xue, and C.-Y.-D. Sim, "Novel pattern-diversity-based decoupling method and its application to multielement MIMO antenna," *IEEE Trans. Antennas Propag.*, vol. 66, no. 10, pp. 4976–4985, Oct. 2018.
- [20] H. Li, B. K. Lau, Z. Ying, and S. He, "Decoupling of multiple antennas in terminals with chassis excitation using polarization diversity, angle diversity and current control," *IEEE Trans. Antennas Propag.*, vol. 60, no. 12, pp. 5947–5957, Dec. 2012.
- [21] J. Ghosh, D. Mitra, and S. Das, "Mutual coupling reduction of slot antenna array by controlling surface wave propagation," *IEEE Trans. Antennas Propag.*, vol. 67, no. 2, pp. 1352–1357, Feb. 2019.
- [22] J.-Y. Lee, S.-H. Kim, and J.-H. Jang, "Reduction of mutual coupling in planar multiple antenna by using 1-D EBG and SRR structures," *IEEE Trans. Antennas Propag.*, vol. 63, no. 9, pp. 4194–4198, Sep. 2015.
- [23] Z. Wang, L. Zhao, Y. Cai, S. Zheng, and Y. Yin, "A meta-surface antenna array decoupling (MAAD) method for mutual coupling reduction in a MIMO antenna system," *Sci. Rep.*, vol. 8, no. 1, Feb. 2018, Art. no. 3152.
- [24] L. Si, H. Jiang, X. Lv, and J. Ding, "Broadband extremely close-spaced 5G MIMO antenna with mutual coupling reduction using metamaterial-inspired superstrate," *Opt. Express*, vol. 27, no. 3, pp. 3472–3482, 2019.
- [25] F. Liu, J. Guo, L. Zhao, X. Shen, and Y. Yin, "A meta-surface decoupling method for two linear polarized antenna array in sub-6 GHz base station applications," *IEEE Access*, vol. 7, pp. 2759–2768, 2019.
- [26] A. Jafarholi, A. Jafarholi, and J. H. Choi, "Mutual coupling reduction in an array of patch antennas using CLL metamaterial superstrate for MIMO applications," *IEEE Trans. Antennas Propag.*, vol. 67, no. 1, pp. 179–189, Jan. 2019.
- [27] F. Liu, J. Guo, L. Zhao, G.-L. Huang, Y. Li, and Y. Yin, "Dual-band metasurface-based decoupling method for two closely packed dual-band antennas," *IEEE Trans. Antennas Propag.*, vol. 68, no. 1, pp. 552–557, Jan. 2020.
- [28] X.-J. Zou, G.-M. Wang, Y.-W. Wang, and H.-P. Li, "An efficient decoupling network between feeding points for multielement linear arrays," *IEEE Trans. Antennas Propag.*, vol. 67, no. 5, pp. 3101–3108, May 2019.
- [29] K.-F. Tong, K.-M. Luk, K.-F. Lee, and R. Q. Lee, "A broad-band U-slot rectangular patch antenna on a microwave substrate," *IEEE Trans. Antennas Propag.*, vol. 48, no. 6, pp. 954–960, Jun. 2000.
- [30] D. R. Smith, S. Schultz, P. Markoš, and C. M. Soukoulis, "Determination of effective permittivity and permeability of metamaterials from reflection and transmission coefficients," *Phys. Rev. B, Condens. Matter*, vol. 65, no. 19, Apr. 2002, Art. no. 195104.
- [31] A. O. Karilainen, P. M. T. Ikonen, C. R. Simovski, and S. A. Tretyakov, "Choosing dielectric or magnetic material to optimize the bandwidth of miniaturized resonant antennas," *IEEE Trans. Antennas Propag.*, vol. 59, no. 11, pp. 3991–3998, Nov. 2011.
- [32] X. Chen, P.-S. Kildal, J. Carlsson, and J. Yang, "MRC diversity and MIMO capacity evaluations of multi-port antennas using reverberation chamber and anechoic chamber," *IEEE Trans. Antennas Propag.*, vol. 61, no. 2, pp. 917–926, Feb. 2013.
- [33] D. M. Pozar, "A relation between the active input impedance and the active element pattern of a phased array," *IEEE Trans. Antennas Propag.*, vol. 51, no. 9, pp. 2486–2489, Sep. 2003.